Persistent discrepancy between experimental and theoretical lifetimes for Ni⁻

R. Si,[1,2] C. Y. Zhang,[1] K. Yao,[1] T. Brage,[2,*] C. Y. Chen,[1,†] and Y. M. Zou[1]

[1]*Shanghai EBIT Lab, Institute of Modern Physics, Department of Nuclear Science and Technology,*
Fudan University, Shanghai 200433, China

[2]*Division of Mathematical Physics, Department of Physics, Lund University, Box 118, SE-221 00 Lund, Sweden*

Recently the lifetime of the excited $3d^9 4s^2\, ^2D_{3/2}$ in Ni⁻ was measured to be 15.1 ± 0.4 s [Phys. Rev. A **93**, 012512 (2016)]. This deviates from results from nonrelativistic, within the LS-approximation, calculations for this forbidden magnetic-dipole transition of 18.88 s [J. Phys. B **50**, 025001 (2017)]. We here present elaborate and fully relativistic multiconfiguration Dirac–Hartree–Fock calculations, to explore this difference. Our calculated transition energy 1485.65 cm⁻¹ is in excellent agreement with the experimental 1485 ± 3 cm⁻¹ [Phys. Rev. A **58**, 2051 (1998)]. However the lifetime of 18.86 s, while agreeing well with the nonrelativistic analytical value, deviates from experiment by 25%. The uncertainties of our calculated wavelength and lifetime are estimated to be better than 0.1% and 1%, respectively. In spite of including a careful investigation of contributions from correlation as well as higher-order relativistic effects, we cannot find any explanation from the structure theory for this deviation.

I. INTRODUCTION

Negative ions are extreme atomic systems, where the binding of the "extra" electron is often only represented by including a careful and involved treatment of electron correlation in calculations. At the same time, the negative ions present us with the least relativistic system in their isoelectronic sequence (i.e., systems with a given number of electrons). Therefore, they will be the system with the most pure LS-coupled structure in the sequence which, as we see below, will actually make some properties easier to predict.

It is well established that negative atomic ions play important roles in many branches of physics, such as astrophysics and atmospheric and plasma physics [1–3], as well as being important in advanced analytical methods [3,4].

Since there is no long-range Coulomb interaction between the outermost electron and the atomic core, negative ions will only have a few bound states. Only in three confirmed cases; namely, Os⁻ [5–7], Ce⁻ [8,9], and La⁻ [10,11] there are excited bound states of opposite parity to the ground state. These are therefore proposed as candidates for laser cooling. In most cases all bound states have the same parity or even belong to the same electron configuration [3,12–14], implying that the leading component for transitions would be forbidden transitions, most prominently magnetic dipole ($M1$) ones. In pure LS-coupling these are easy to compute, and therefore show a stable behavior as a function of the complexity of our calculations. As a matter of fact, the transition rate of these transitions will not depend on the wave function directly, but only on the energy difference between the levels involved in the transition (see Ref. [15] and references therein). These somewhat contra-intuitive properties, where the transition energy is a challenge to theory, while the rate is straightforward to calculate, is accentuated for the anionic systems. In a relativistic approach things are more complex. The final wave function will be a mixture of different LS terms and the line strength will depend on the energy difference. When introducing QED effects, the anomalous magnetic moment g_s will also affect the value of the line strength. This was addressed in recent work by Froese Fischer and co-workers [16,17]. As was shown in these papers, these effects are expected to be negligible, especially for the nonrelativistic limit represented by negative ions.

In this paper we address a discrepancy between theory and experiment for Ni⁻ regarding the transition rate [15], where the analytic LS theory disagrees with experiment [18] by around 25%. This discrepancy is about an order of magnitude larger than the stated experimental uncertainty estimates (about 2%–3%). We will therefore investigate and probe possible contributions to this rate to see if the reason for this discrepancy could be explained.

II. METHOD OF CALCULATIONS—WAVE FUNCTIONS

In this paper we use the relativistic multiconfiguration Dirac–Hartree–Fock (MCDHF) method, in the form of the GRASP2K package [19] to model the negative ions. This method was recently used to predict electron affinities for several elements [20,21]. The use of a fully relativistic approach might appear as somewhat overambitious, since the negative ions do not exhibit strong relativistic effects. However, as we will see, the only explanation to the deviation between theory and experiment for the transition rate can be found in relativistic contributions, through deviation from the simple behavior for pure LS coupling. By using the MCDHF method we choose the opposite extreme in the coupling scheme, the jj coupling, and thereby virtually include the effect of all relevant LS terms.

We represent the negative ion by an atomic state function (ASF) $\Psi(\Gamma J)$, which is expanded in a linear combination of configuration state functions (CSFs) $\Phi(\gamma_i J)$:

$$\Psi(\Gamma J) = \sum_{i=1}^{N} c_i \Phi(\gamma_i J), \qquad (1)$$

*tomas.brage@fysik.lu.se
†chychen@fudan.edu.cn

where γ_i represents all other quantum numbers needed to uniquely define the CSF, and Γ is usually set as the γ_i for the $\Phi(\gamma_i J)$ with the largest weight c_i^2. The CSFs are spin-angular coupled, antisymmetric products of Dirac orbitals of the form

$$\phi(\mathbf{r}) = \frac{1}{r}\begin{pmatrix} P_{n\kappa}(r)\chi_{\kappa m}(\theta,\phi) \\ i\,Q_{n\kappa}(r)\chi_{\kappa m}(\theta,\phi) \end{pmatrix}, \qquad (2)$$

where we use standard notations. The radial part of the orbitals are determined by solving the MCDHF equations, which are variationally derived from the Schrödinger equation

$$H\Psi = E\Psi, \qquad (3)$$

where H is defined as the Dirac–Coulomb Hamiltonian during the variational calculations. Breit and QED corrections are later introduced in a relativistic configuration interaction (RCI) type of calculation, without changing the orbitals. The radial part of the orbitals are defined as "numerical", on a grid.

The CSFs are generated by allowing for excitation from a reference set of CSFs to an active set of orbitals. In the present case of the Ni$^-$ ground state, the reference set is defined as the $1s^2 2p^6 3s^2 3p^6 3d^9 4s^2$ configuration, where we use the nonrelativistic notation, where each nl represents two relativistic orbitals (except for ns); namely, $nl_{j=l-1/2}$ and $nl_{j=l+1/2}$. This configuration includes two atomic states for $J = 5/2$ and $3/2$. By increasing the active set, layer by layer, we will be able to monitor our calculations for convergence. We also can change the model to open up for more excitations. This can be done in two dimensions. First, we might allow for excitations from ever deeper subshells, thereby probing the inner parts of the ion. We will in the present calculations probe for contributions to correlation from all occupied core subshells. Second, we can also allow for different number of excitations from the different subshells. If we define the $3d^9 4s^2$ as our valence part of the ion, all other subshells are core subshells. We will allow for single and double excitations and therefore we can distinguish between three different sorts of correlation:

(1) VV correlation (valence-valence), where we allow for single and double excitations from only the outermost two open subshells;

(2) CV correlation (core-valence), where we allow for at the most a single excitation from the core subshells;

(3) CC correlation (core-core), where we allow for double excitations from the core subshells.

We will through these definitions define both a set of models, which probes important correlations, and a set of calculations within the models, with increasing active sets, that probes the convergences within the models.

A. Valence-valence correlation

In our first set of VV calculations, we use $3d^9 4s^2\,^2D_{3/2,5/2}$ as the reference set and CSFs are generated by keeping the core electrons ($1s^2 2s^2 2p^6 3s^2 3p^6$) inactive and allowing for single and double (SD) excitations of the valence orbitals in the reference configurations to orbitals in the active set with $n \leqslant 7$ and $l \leqslant (n-1)$.

One possible objection to this approach is the fact that the reference set, from which we make our excitations, is too small. It is often important to include more than one CSF in

this set to allow for the most important triple excitations. It is to be expected that members of the Layzer complex [22] should contribute with large weight and we notice that, for the two bound levels of Ni$^-$, other than the overwhelmingly dominant CSFs $3d^9 4s^2\,^2D_{3/2,5/2}$ with expansion coefficients of about 91%, the CSFs with the next largest expansion coefficients of about 1% belong to the $3d^9 4p^2$ configuration. The effect on the energy splitting was relatively large (about 30.8 cm^{-1}) but it did not affect the line strength (see Table I). As a matter of fact, the effect of including a multireference set is larger than the effect of including CV or CC in our calculations.

B. Separate core-valence and separate core-core tests

The inclusion of CV and CC correlation is a challenge, since the size of the CSF expansion will increase fast with the size of the active set. We will therefore start by probing the importance of the correlation with and within different core subshells by using what we label as separate CV and CC (SCV and SCC) [23–25]. In this way we do separate CV and CC calculations for all core subshells, down to and including the $1s$, to explore the importance of different core correlation contributions. We use the same reference set and form of the active set as in the different steps in the VV calculations. The resulting energy splittings, line strengths, transition rates for the $M1$ transition $3d^9 4s^2\,^2D_{3/2} \rightarrow 3d^9 4s^2\,^2D_{5/2}$, as well as the lifetimes for $3d^9 4s^2\,^2D_{3/2}$ are listed in Table I. Here we only include the $M1$ transition rate, since the $E2$ transition rate is about five orders of magnitude smaller.

Other than our *ab initio* calculated results, the adjusted transition rates and lifetimes, which are rescaled with experimental energies according to

$$A_{\text{adjusted}} = \left(\frac{E_{\text{expt}}}{E_{\text{ab initio}}}\right)^3 A_{\text{ab initio}}, \qquad (4)$$

and

$$\tau_{\text{adjusted}} = \frac{1}{A_{\text{adjusted}}}, \qquad (5)$$

are also listed in Table I.

C. Final core valence

From the experiences gained by the exploratory and separate calculations labeled SCV and SCC, together with the effect of including a multireference set (MR), we designed a "final" and "full" core valence model, labeled FCV. We here balance a reasonable complexity with the attempt to include all important effects.

The starting point is the variational part of the calculations, where, through an iterative procedure, we obtain the radial functions for our orbitals. In this we use only the $3d^9 4s^2$ as the reference configuration and include VV as well as CV correlation with $3p$ and $3s$ subshells, through SD substitutions with orbitals in active sets up to $n = 9$ and $l = 7$.

We follow this with a configuration-interaction calculation, usually labeled RCI, without optimizing the orbitals. In this we used a multireference set consisting of the $\{3d^9 4s^2, 3d^9 4p^2\}$ configurations. We now allow for, in additions to what was included in the variational calculations above, SD

TABLE I. Energies E (in cm^{-1}), line strengths S (in atomic units), and transition rates A (in s^{-1}) for the $3d^9 4s^2 \, ^2D_{3/2} \rightarrow 3d^9 4s^2 \, ^2D_{5/2}$ transition, together with lifetime τ (in s) of the $3d^9 4s^2 \, ^2D_{3/2}$, from different correlation models. For the MR, SCV, and SCC models, we list differences from the VV results—for energies in absolute values, for S and A the percentages. For the FCV we list the final results. "LS" represents the analytical results in the LS limit (see text). EXPT is the measured values (from Refs. [13] and [18]).

Method	Ab initio			Adjusted		
	E	S	A	τ	A	τ
Calculations without CV or CC:						
DF	1426.06	2.399	0.04691	21.32	0.05297	18.88
VV(SR)	1475.67	2.398	0.05197	19.24	0.05296	18.88
VV(MR)	-30.79%	-0.0042%	-6.13%	20.50	0.05296	18.88
Separate and exploratory calculations:						
SCV$_{3p}$	12.97	0.0042%	2.67%	18.74	0.05296	18.88
SCC$_{3p}$	-0.06	0.0000%	-0.012%	18.75	0.05296	18.88
SCV$_{3s}$	-3.43	0.0033%	-0.69%	19.38	0.05296	18.88
SCC$_{3s}$	0.63	0.0000%	0.13%	19.65	0.05296	18.88
SCV$_{2p}$	15.55	0.0054%	3.20%	18.65	0.05296	18.88
SCC$_{2p}$	-15.37	0.0038%	-3.06%	19.23	0.05297	18.88
SCV$_{2s}$	-1.2	0.0025%	-0.24%	19.29	0.05296	18.88
SCC$_{2s}$	3.63	0.0017%	0.74%	19.15	0.05296	18.88
SCV$_{1s}$	0.03	0.0000%	0.01%	19.24	0.05296	18.88
SCC$_{1s}$	-1.07	0.0008%	0.22%	19.28	0.05296	18.88
Final results:						
FCV	1485.65	2.398	0.05303	18.86	0.05296	18.88
LS		2.400			0.05297	18.88
EXPT	1485 ± 3					15.1 ± 0.4

excitations from the $3d$, $4s$, and $4p$ subshells of the reference configurations, to active sets up to $n = 9$ and $l = 7$. From these reference configurations we also included single substitutions from the $3p$ and $3s$ subshells to active sets up to $n = 6$ and $l = 5$, to represent the CV contributions from these subshells. For the $n = 9$ expansion, this results in a total of 1 167 866 and 1 617 467 CSFs for $J = 3/2$ and $J = 5/2$, respectively.

D. Breit and quantum electrodynamics effects

We monitor the effect of the Breit interaction and QED (self-energy and vacuum polarization) corrections all through our calculations. It turns out that, when using the standard GRASP2K approximation [19], the Breit interaction reduces the energy splitting between $3d^9 4s^2 \, ^2D_{3/2}$ and $^2D_{5/2}$ by about 121 cm^{-1}, while QED effect widens it by about 2 cm^{-1}. On the other hand, the line strength for the $M1$ transitions is not affected by including these effects. We can conclude that these effects therefore do not influence the admixture of CSF that would break the leading LS composition of the wave function.

III. METHOD OF CALCULATIONS—ANALYTICAL LINE STRENGTHS

In this paper we present results for line strengths from involved MCDHF calculations, but as was pointed out recently [15] in pure LS coupling, the $M1$ transition rates are trivial to compute. The "analytical" line strengths are then given by [26]

$$S_{LS} \approx |\langle ^2D_{5/2}||\mathbf{J}^{(1)} + (g_s - 1)\mathbf{S}^{(1)}||^2D_{5/2}\rangle|^2 \approx \tfrac{12}{5}. \quad (6)$$

The rate is then given by

$$A_{LS} \approx \frac{2.6973 \times 10^{-11}\sigma^3}{4} S_{LS} \approx 1.6184 \times 10^{-11}\sigma^3, \quad (7)$$

and an LS value for the lifetime would be

$$\tau_{LS} = \frac{1}{A_{LS}} \approx \frac{6.1789 \times 10^{10}}{\sigma^3}. \quad (8)$$

In all these, σ is given in cm^{-1}, rates in s^{-1}, and lifetimes in s. These values are also given in Table I for comparison.

Deviation in our calculations from this simple, analytical model could be due to several effects. First, we might expect deviations from the LS approximations, where mixing of other terms than ^2D contributes. Second, the line strength for $M1$ transitions is only independent to first order of the wavelength in a relativistic approach. Higher-order effects could influence the final result. Third, the anomalous contribution to the magnetic moment is not included, i.e., we are not considering the effect of $g_s \neq 2$. The latter two effects are expected to be small and negligible in the case of Ni$^-$ [17].

IV. RESULTS AND DISCUSSIONS

It is clear from Table I that the $M1$ line strength is almost independent of our approach, since the fluctuations of its value are within 0.006%. In spite of our attempts to test all possible reasons for deviations from the nonrelativistic result, we see no sign of any tendency to deviate substantially from the "analytical" value of 2.4 a.u. for the line strength.
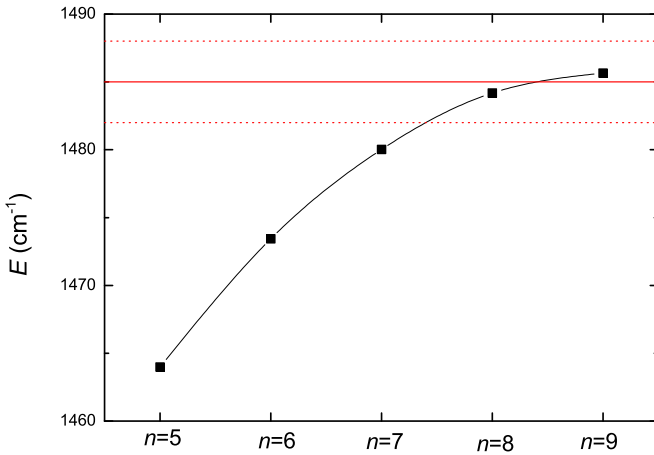
FIG. 1. Transition energy for $3d^9 4s^2 \, ^2D_{3/2} \rightarrow 3d^9 4s^2 \, ^2D_{5/2}$ as a function of maximum principle quantum number of the active sets. The horizontal solid line represents the experimental result, while the dashed lines represent the experimental error [13].

The transition energy is a true challenge for theory, which is illustrated by the different results in Table I. There are contribution to this fine-structure splitting from correlation including deep core subshells and, as a matter of fact, the $2p$ CV contribution is larger than from $3p$. This is in accordance with our previous study of $3d^9$ Co-like cations [25]. However, the $2p$ and $3p$ CV contributions have opposite effects in Co-like cations; here both of them enlarge the energy splitting. On the other hand, the contributions from all the CC correlations are small in Co-like cations, but as seen from Table I, the contribution from the $2p$ CC correlation is almost the same as CV contribution from the same subshell, but with opposite sign, leading to an almost complete cancellation. The effect on the fine structure from deep shells has also been observed in Ag-like systems [24]. It is clear that it is mainly an indirect effect on the size of the Breit interaction, which increases when core subshells are opened. This could in turn be attributed to us not including this operator in the variational procedure.

Our final FCV results are listed in Table I. The transition energy is in excellent agreement with experiment, but an important final test is of course the convergence of the calculations. We represent this in Fig. 1, where we show the energy of the $3d^9 4s^2 \, ^2D_{3/2} \rightarrow 3d^9 4s^2 \, ^2D_{5/2}$ transition as a function of the maximum principal quantum number n of the active set, and thereby the size of our calculations. It is clear that the calculations converge, within the model. We estimate from this convergence study that the uncertainty of our computed transition energy is about 0.1%. From Table I we can also argue that our model includes all important contributions. It is therefore fair to assume that the uncertainty in our final result should be of the same order of magnitude, or less, as the experimental error estimate of 0.2%.

V. CONCLUSION

Our final calculated and well-converged (0.1%) wave number 1485.65 cm^{-1} is in excellent agreement with the experimental measurement 1485 ± 3 cm^{-1} [13]. However, the computed lifetime for $3d^9 4s^2 \, ^2D_{3/2}$ is 18.86 s, which agrees well with the analytical value of 18.88 s [15], but shows a significant difference from the experimental value of 15.1 ± 0.4 s [18]. The computed line strength in our fully relativistic approach should be converged to within 0.1%, since both correlation and higher-order relativistic effects have been explored. Due to the good convergence of our calculated wavelength and line strength, the deviation of our calculation from LS coupling, the uncertainty in our estimated lifetime is expected to be well within 1%. The discrepancy by about 25% from the experimental lifetime remains unexplained.

[1] S. J. Buckman and C. W. Clark, Rev. Mod. Phys. **66**, 539 (1994).

[2] T. Andersen, Phys. Rep. **394**, 157 (2004).

[3] D. J. Pegg, Rep. Prog. Phys. **67**, 857 (2004).

[4] L. K. Fifield, Rep. Prog. Phys. **62**, 1223 (1999).

[5] R. C. Bilodeau and H. K. Haugen, Phys. Rev. Lett. **85**, 534 (2000).

[6] U. Warring, M. Amoretti, C. Canali, A. Fischer, R. Heyne, J. O. Meier, C. Morhard, and A. Kellerbauer, Phys. Rev. Lett. **102**, 043001 (2009).

[7] A. Fischer, C. Canali, U. Warring, A. Kellerbauer, and S. Fritzsche, Phys. Rev. Lett. **104**, 073004 (2010).

[8] C. W. Walter, N. D. Gibson, C. M. Janczak, K. A. Starr, A. P. Snedden, R. L. Field, and P. Andersson, Phys. Rev. A **76**, 052702 (2007).

[9] C. W. Walter, N. D. Gibson, Y. G. Li, D. J. Matyas, R. M. Alton, S. E. Lou, R. L. Field, D. Hanstorp, L. Pan, and D. R. Beck, Phys. Rev. A **84**, 032514 (2011).

[10] C. W. Walter, N. D. Gibson, D. J. Matyas, C. Crocker, K. A. Dungan, B. R. Matola, and J. Rohlen, Phys. Rev. Lett. **113**, 063001 (2014).

[11] E. Jordan, G. Cerchiari, S. Fritzsche, and A. Kellerbauer, Phys. Rev. Lett. **115**, 113001 (2015).

[12] H. Hotop and W. C. Linebeger, J. Phys. Chem. Ref. Data **14**, 731 (1985).

[13] M. Scheer, C. A. Brodie, R. C. Bilodeau, and H. K. Haugen, Phys. Rev. A **58**, 2051 (1998).

[14] T. Andersen, H. K. Haugen, and H. Hotop, J. Phys. Chem. Ref. Data **28**, 1511 (1999).

[15] T. Brage and J. Grumer, J. Phys. B: At., Mol. Opt. Phys. **50**, 025001 (2017).

[16] N. D. Guise, J. N. Tan, S. M. Brewer, C. F. Fischer, and P. Jönsson, Phys. Rev. A **89**, 040502(R) (2014).

[17] C. F. Fischer, I. P. Grant, G. Gaigalas, and P. Rynkun, Phys. Rev. A **93**, 022505 (2016).

[18] M. Kaminska, V. T. Davis, O. M. Hole, R. F. Nascimento, K. C. Chartkunchand, M. Blom, M. Bjorkhage, A. Kallberg, P. Lofgren, P. Reinhed, S. Rosen, A. Simonsson, R. D. Thomas, S. Mannervik, P. A. Neill, J. S. Thompson, H. T. Schmidt, H. Cederquist, and D. Hanstorp, Phys. Rev. A **93**, 012512 (2016).

[19] P. Jönsson, G. Gaigalas, J. Bieroń, C. F. Fischer, and I. Grant, Comput. Phys. Commun. **184**, 2197 (2013).

[20] J. Li, Z. Zhao, M. Andersson, X. Zhang, and C. Chen, J. Phys. B: At., Mol. Opt. Phys. **45**, 165004 (2012).

[21] J. Li, Z. Zhao, and X. Zhang, Europhys. Lett. **107**, 33001 (2014).

[22] C. F. Fischer, M. Godefroid, T. Brage, P. Jönsson, and G. Gaigalas, J. Phys. B: At., Mol. Opt. Phys. **49**, 182004 (2016).

[23] Z. Fei, R. Zhao, Z. Shi, J. Xiao, M. Qiu, J. Grumer, M. Andersson, T. Brage, R. Hutton, and Y. Zou, Phys. Rev. A **86**, 062501 (2012).

[24] J. Grumer, R. Zhao, T. Brage, W. Li, S. Huldt, R. Hutton, and Y. Zou, Phys. Rev. A **89**, 062511 (2014).

[25] X. L. Guo, R. Si, S. Li, M. Huang, R. Hutton, Y. S. Wang, C. Y. Chen, Y. M. Zou, K. Wang, J. Yan, C. Y. Li, and T. Brage, Phys. Rev. A **93**, 012513 (2016).

[26] R. D. Cowan, *The Theory of Atomic Structure and Spectra* (University of California Press, Berkeley, 1981).